Hydrogen chemisorption on singly vanadium doped aluminum clusters

Jan Vanbuel[a], Eva M. Fernández[b], Piero Ferrari[a], Sandy Gewinner[c], Wieland Schöllkopf[c], Luis C. Balbás[d], André Fielicke[c, e], and Ewald Janssens*[a]

Abstract: *The effect of vanadium doping on the hydrogen adsorption capacity of aluminum clusters (Al_n^+, n = 2–18) is studied experimentally by mass spectrometry and infrared multiple photon dissociation (IRMPD) spectroscopy. We find that vanadium doping enhances the reactivity of the clusters towards hydrogen, albeit in a size-dependent way. IRMPD spectra, which provide a fingerprint of the hydrogen binding geometry, show that H_2 dissociates upon adsorption. Density functional theory (DFT) calculations for the smaller Al_nV^+ (n = 2 – 8,10) clusters are in good agreement with the observed reactivity pattern and underline the importance of activation barriers in the chemisorption process. Orbital analysis shows that the activation barriers are due to an unfavorable overlap between cluster and hydrogen orbitals.*

With an ever-growing global energy consumption, the need for a more sustainable and environment-friendly alternative to our use of fossil fuels becomes increasingly dire. Di-hydrogen, H_2, with a gravimetric energy density roughly three times that of gasoline[1], is one such alternative and has been the subject of extensive study[2–4]. A major drawback, however, is the low volumetric energy density of gaseous hydrogen, which urges for other means of storage. For mobile applications, the requirements posited by the U.S. Gov. Department of Energy are rather stringent; by 2020, hydrogen storage materials should have at least 5.5 wt% and 40 gL^{-1} volumetric capacity, with operating and recharging conditions around ambient temperature and pressure. Nanostructured materials are prospective in this regard[5–7], but as of yet not economically viable. To eventually device storage media superior to what is currently available, a better understanding of the interaction between hydrogen and potential storage materials is highly desirable. Nanoclusters, whose physico-chemical properties are strongly size-dependent and therefore exhibit a multitude of chemically distinct and possibly reactive sites, are useful model systems for designing more efficient storage media on a larger scale. By studying these clusters in the well-defined experimental conditions (cluster size and composition, charge state) that are characteristic of gas-phase experiments[8], one gains more insight in the kinetics and dynamics of hydrogenation reactions of nanostructured materials, which could pave the way towards a sustainable hydrogen economy.

Aluminum, one of the lightest and most abundant metals on earth, is known to form the bulk metal hydrides alane, AlH_3, and sodium alanate, $NaAlH_4$, which have a hydrogen weight percentage of 10% and 5.6%, respectively. Despite unremitting efforts[9,10], the slow hydrogenation kinetics of both materials limits their use for practical purposes. The bottleneck in the hydrogenation process is a high activation barrier (of the order of 1 eV) in the dissociative reaction pathway, a barrier which is present for bulk as well as small clusters of aluminum[11–14]. Several computational studies have shown that doping aluminum with transition metals such as Ti, Cr, V, Co, … lowers the activation barriers towards dissociative chemisorption[15–18]. For vanadium doped aluminum clusters, experimental confirmation of the predicted[18] size-dependent reactivity is limited[19] and a detailed description of the role of vanadium in the reaction is still lacking. In this work, we study the reactivity of singly vanadium doped aluminum clusters towards hydrogen by means of mass spectrometry and infrared multiple photon dissociation spectroscopy (IRMPD). For the smaller sizes, we compare density functional theory calculations with the experimental data to rationalize our observations.

Figure 1 shows a mass spectrum of $Al_nV_m^+$ ($n = 1-18, m = 0-3$) clusters, before (Fig. 1a) and after (Fig. 1b) interaction with H_2. The distributions of bare clusters (i.e. $Al_nV_m^+$ without hydrogen) for $m = 0, 1, 2$ are designated by colored lines. After injecting H_2 into the source, the undoped aluminum cluster distribution (red line) barely changes. For the single (blue line) and double (green line) vanadium doped clusters, an overall decrease in abundance indicates that a fraction of the clusters has reacted with hydrogen to form hydrogen complexes. A zoom of part of the hydrogenated mass spectrum is shown in Fig. 1c. In this letter, the scope of the analysis will be limited to the singly vanadium doped aluminum clusters, the most abundant species in the mass spectra. For these clusters, the fractional distribution of the hydrogenated complexes can be extracted from the mass spectra:

$$[\mathrm{Al}_n\mathrm{VH}_{2p}{}^+]_{frac} = \frac{\mathrm{I}(\mathrm{Al}_n\mathrm{VH}_{2p}{}^+)}{\sum_{i=0}^{2}\mathrm{I}(\mathrm{Al}_n\mathrm{VH}_{2i}{}^+)}, \quad (1)$$

with $\mathrm{I}(\mathrm{Al}_n\mathrm{VH}_{2p}{}^+)$ the intensity of the cluster species in the mass spectra. This fractional distribution is plotted in Fig. 1d.

[a] Prof. Dr. Ewald Janssens, Jan Vanbuel, Piero Ferrari
Laboratory of Solid State Physics & Magnetism
KU Leuven
Celestijnenlaan 200D, 3001 Leuven, Belgium
E-mail: ewald.janssens@kuleuven.be
[b] Dr. Eva Fernández
Departamento de Física Fundamental
UNED
Paseo Senda del Rey 9, 28040 Madrid, Spain
[c] Dr. Wieland Schöllkopf, Sandy Gewinner
Fritz-Haber-Institut der Max-Planck-Gesellschaft
Faradayweg 4–6, 14195 Berlin, Germany
[d] Prof. Dr. Luis Balbás
Departamento de Física Teórica
Universidad de Valladolid
Paseo Belén 7, 47011 Valladolid, Spain
[e] Prof. Dr. André Fielicke
Institut für Optik und Atomare Physik
TU Berlin
Hardenbergstraße 36, 10623 Berlin, Germany

Supporting information for this article is given via a link at the end of the document.

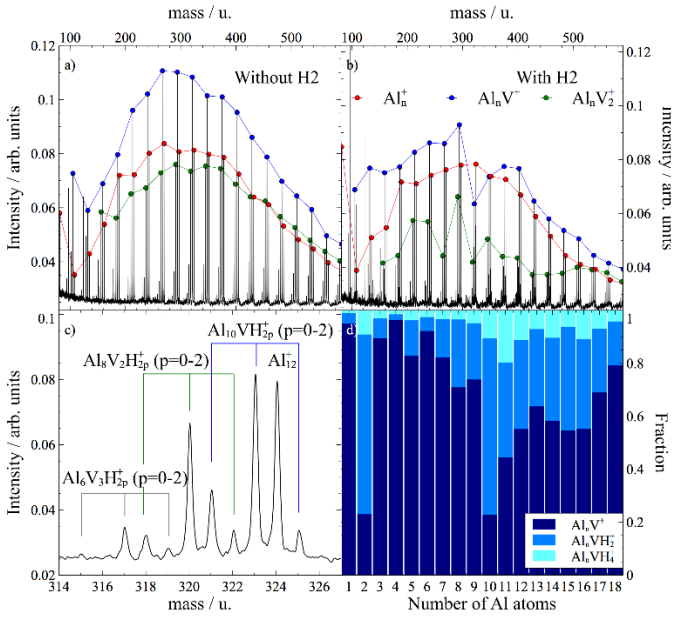

Figure 1. Parts of mass spectra of $Al_nV_m^+$ (n = 1-18, m = 0-2) clusters, a) before and b) after interaction with H_2. c) Zoom of a part of the mass spectrum after interaction with H_2 shows the presence of hydrogenated complexes. d) Fractional distribution of hydrogenated Al_nV^+ (n = 1-18) clusters.

Doping pure aluminum clusters with one vanadium atom changes the clusters' reactivity in a size-dependent way: small Al_nV^+ clusters (n = 1–9) are relatively unreactive towards H_2, with the exception of Al_2V^+. Significantly larger reactivities are observed for medium sized clusters (n = 10–16). Especially $Al_{10}V^+$ exhibits a drastically increased reactivity. For clusters larger than n = 16 the reactivity decreases again. Experimental work by Lang et al.[20] suggested that after n = 16, the position of the vanadium dopant in the Al_nV^+ clusters changes from an exohedral to an endohedral site. This structural transformation hypothesis was confirmed by computational work of Fernandez et al.[21] The observed decrease in reactivity for the larger sizes then, is in line with the assumption that the vanadium dopant acts as a reactive center for H_2 adsorption: for clusters of size larger than $Al_{16}V^+$, the vanadium dopant becomes shielded by a cage of aluminum atoms, thereby impeding the interaction with H_2.

A priori, it is not clear whether the hydrogen molecule dissociates upon adsorption or not. Additionally, the observation that the amount of adsorbed hydrogen molecules is limited to mostly one for single doped aluminum clusters could imply that the vanadium atom, which is considered to be the active site[22,23], gets poisoned after interaction with the first hydrogen molecule. A tentative answer to both questions can be found by analysis of the IRMPD spectra of the hydrogenated clusters, which provide a fingerprint of the hydrogen binding geometry. A detailed description of this technique can be found in Ref.[24] and a shorter version is included in the supporting information (SI). In figure 2, several low-energy configurational isomers of $Al_{10}VH_2^+$ are plotted together with the experimental and their calculated IR spectra. The spectrum of the putative ground state isomer shows good agreement with the experimental data, although the positions as well as the intensities of a second, almost degenerate isomer ($\Delta E = 0.003\ eV$) provide an even better match. If there is no considerable energy barrier separating them, both isomers could be present in the molecular beam. The next higher isomer ($\Delta E = 0.12\ eV$) can be excluded because of the absence of the band at ~1900 cm $^{-1}$. For the fourth isomer ($\Delta E = 0.17\ eV$), the calculated bands are at lower wavenumbers than the experimental ones, and the intensities don't agree well with the experiment. Moreover, the metal framework of iso3 and iso4 differs significantly in structure from the calculated bare cluster (SI), whereas that of the tentative ground state iso1 and of iso2 are very similar.

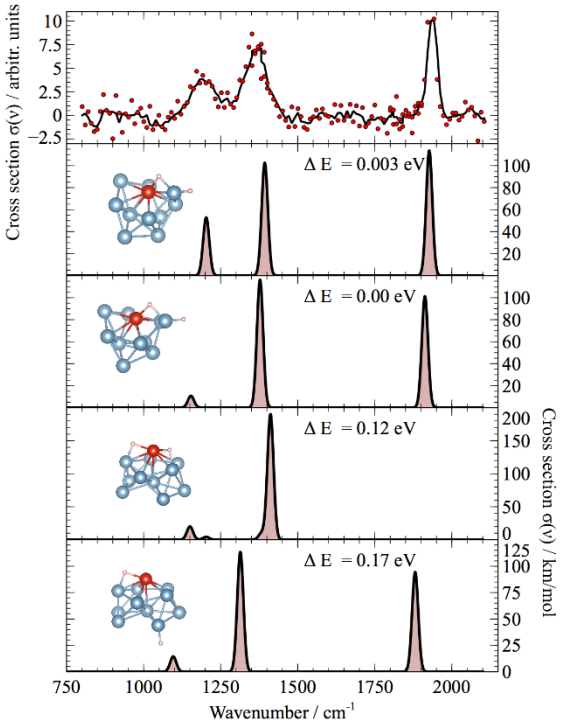

Figure 2. Experimental IRMPD cross section vs. calculated IR intensity for energetically low-lying isomers of $Al_{10}VH_2^+$ (Blue = Al, red = V, white = H). The upper panel contains the experimental data points in red, together with a three-point running average in black. The lower panels show the calculated harmonic IR spectra of four low-energy configurational isomers. The discrete resonances are artificially broadened by 10 cm^{-1} to facilitate comparison with the experimental data.

The bands observed in the 800 – 2100 cm^{-1} region for $Al_{10}V^+$ are related to the stretching modes of atomic hydrogen-metal bonds, meaning that the H_2 molecule dissociates upon adsorption: the feature around 1900 cm^{-1}, for example, corresponds to the stretching mode of a hydrogen atom bound on-top position of an aluminum atom; the bands at approximately 1350 cm^{-1} and 1240 cm^{-1} correspond to the symmetric and asymmetric stretch of a hydrogen bound in a bridge position between a vanadium and an aluminum atom and the frequencies are similar to those for hydrogen bound dissociatively to transition metal (Fe, Co, V and Ni) clusters[25]. For all calculated isomers of $Al_{10}VH_2^+$, one or two of the hydrogen atoms are bound to a vanadium atom, further corroborating the hypothesis that, at least for this size, the vanadium dopant gets poisoned after adsorption. Infrared spectra for larger sizes (n = 11, 12, 13, 15), for which no DFT calculations are available, exhibit spectral features in the same wavenumber regime and are included in the SI. The IR spectra of the few smaller sizes that do adsorb hydrogen, namely Al_nV^+ with n = 2, 8, 9 (see Fig. 1d), do not show any discernible IR bands, which could be due to insufficient oscillator strength of the vibrational resonances to desorb the hydrogen. Another explanation could be that the

Table 1. DFT computational results for selected Al_nV^+ (n = 2-10). For each cluster, the initial and final spin state, as well as the physisorption energy $E_{ads}(H_2)$ and the chemisorption energy $E_{ads}(2H)$ are listed.

Cluster	S_i	$E_{ads}(H_2)$ (eV)	S_f	$E_{ads}(2H)$ (eV)
Al_2V^+	5	0.304	5	1.229
Al_3V^+	6	0.212	4	0.756
Al_4V^+	5	0.260	3	0.898
Al_5V^+	4	0.187	4	0.887
Al_6V^+	3	0.279	3	0.594
Al_7V^+	6	0.315	4	0.941
Al_8V^+	5	0.375	5	0.824
Al_9V^+	4	0.349	4	0.847
$Al_{10}V^+$	1	0.109	1	0.928

hydrogen for these sizes is mainly bound molecularly, in which case the characteristic vibrations are expected to lie outside our measurement range[25,26], i.e. below 800 cm^{-1} (M-(H_2) stretch) and above 2100 cm^{-1} (H-H stretch).

For the smaller Al_nV^+ sizes ($n = 2-10$) DFT calculations show that the hydrogen molecule first physisorbs on top of a vanadium atom in a precursor state before dissociating into its atomic constituents (structures and properties can be found in the supporting information). Table 1 contains calculated properties of selected vanadium doped aluminum clusters, such as the spin state before adsorption (S_i), the physisorption energy ($E_{ads}(H_2)$), the spin state after chemisorption (S_f), and the dissociative chemisorption energy ($E_{ads}(2H)$).

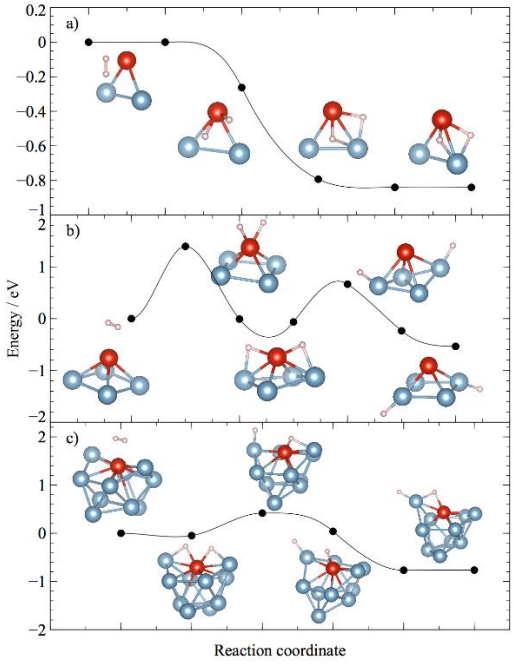

Figure 3. Reaction pathways for the dissociative adsorption of H_2 on a) Al_2V^+, b) Al_4V^+ and c) $Al_{10}V^+$. Initially, at E=0, the hydrogen is still bound molecularly. For Al_2V^+ the reaction is barrierless. For $Al_{10}V^+$, the first step along the reaction coordinate is barrierless, followed by a small diffusion barrier towards the final state. For Al_4V^+, there are two energetic barriers along the reaction coordinate.

The values of $E_{ads}(2H)$ suggest that among the smaller clusters, $Al_2VH_2^+$ is the most stable species and hence is expected to be more abundant in the mass spectra, whereas $Al_6VH_2^+$ should be less abundant. Figure 1d) shows that for Al_2V^+ and Al_6V^+ this argument agrees well with the experiment, but for other sizes the situation is less straightforward; $Al_4VH_2^+$, for example, has a relatively high adsorption energy (0.898 eV), but has a low abundance in the mass spectra. Figure 3 explains the reason for this discrepancy: for Al_2V^+ the H_2 chemisorption reaction occurs barrierless, whereas for Al_4V^+ there is an activation barrier of almost 1.4 eV. In other words, although the formation of $Al_4VH_2^+$ is thermodynamically favorable, it is impeded by the kinetics of the reaction, at least on the timescale of the experiment (i.e. about 100 µs). Fig. 3c shows that for $Al_{10}V^+$ the first step along the reaction coordinate, i.e. the dissociation step of H_2, is barrierless as well, in agreement with its observed abundance in the mass spectra. Calculated pathways for Al_3V^+, Al_6V^+ and Al_8V^+ (SI) show that the dissociative adsorption of hydrogen onto the cluster is also impeded by activation barriers of respectively 0.65, 0.15 and 0.12 eV.

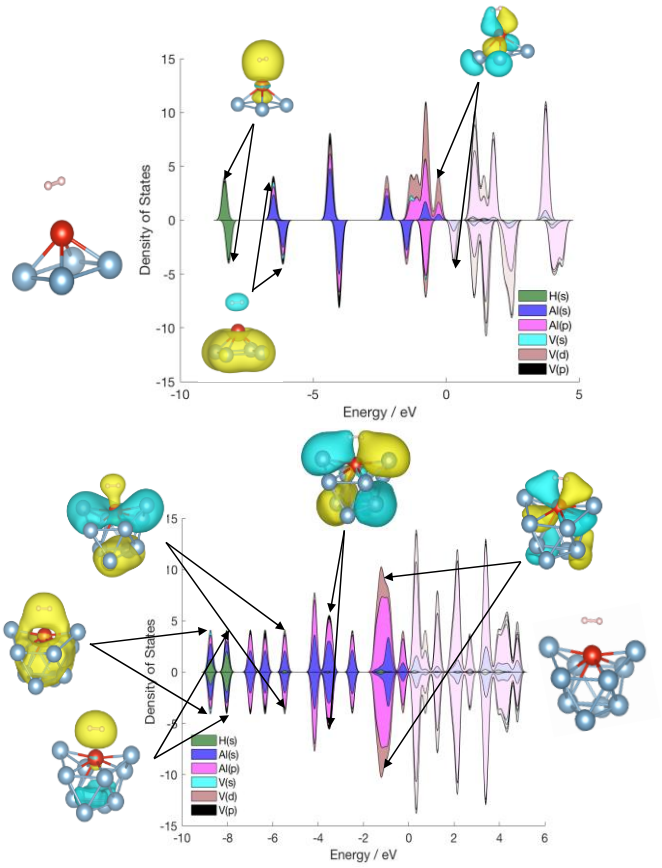

Figure 4. PDOS and selected orbitals of $Al_4V^+ \cdot H_2$ and $Al_{10}V^+ \cdot H_2$.

Analysis of the projected density of states (PDOS) molecular orbitals of the clusters provides insight in the magnitude of these activation barriers. This is illustrated for the complexes with molecularly bound hydrogen $Al_4V(H_2)^+$ and $Al_{10}V(H_2)^+$ in figure 4. Only the orbitals which have a contribution of the hydrogen s-orbitals are indicated in the figure. The deepest bound states for both clusters are formed by the symmetric and anti-symmetric superposition of the doubly occupied H_2-σ orbital with a cluster S-orbital (which, in turn,

consists of the delocalized Al(s) electrons). For $Al_4V^+(H_2)$, there is a singly occupied orbital of mainly d-character near the Fermi energy which has a node in between the hydrogen atoms, i.e. there is back-donation of electronic charge from the cluster into the anti-bonding σ^* orbital of H_2. In contrast, the PDOS and orbitals containing H(s) character of $Al_{10}V^+(H_2)$ show that for this cluster there are two orbitals of anti-bonding character, one located near the Fermi level and one around –4 eV, both of which are doubly occupied. This suggests that the destabilization of the hydrogen-hydrogen bond upon physisorption of the H_2 might be stronger for $Al_{10}V^+$ compared to Al_4V^+, leading to a lower activation barrier in the hydrogenation reaction. Similar orbital features can be observed for other small Al_nV^+ clusters (see supporting information): unreactive clusters ($n = 3, 4, 5, 6, 7, 8$) have at most a singly occupied orbital which overlaps with the σ^* H_2 orbital, whereas reactive ones ($n = 2, 10$) have either two or one doubly occupied orbitals of this kind. The above explanation is similar to the arguments provided by Pino et al.[12] in their computational study explaining the experimentally observed inertness of pure aluminum clusters towards hydrogen[13,14]. Most of the small pure aluminum clusters have a triplet ground state, and the formation of the hydrogenated clusters, which prefer singlet states, is impeded by a large activation barrier along the pathway. The PES of the singlet states, however, which are initially higher in energy than the triplet states ($\Delta E \approx 0.1 - 0.4$ eV), show a smaller and sometimes even negligible barrier. This is explained by double instead of single occupancy of an orbital which is anti-bonding with respect to the H_2 bond for the singlet states. This argument also explains the observed reactivity of Al_6 [14], the only reactive pure aluminum cluster, for which the singlet and triplet state were found to be almost degenerate[12] and with the singlet state even lower in energy in the work of Moc[27].

In summary, the interaction of singly vanadium doped aluminum clusters with molecular hydrogen was studied experimentally by mass spectrometry and infrared multiple photon dissociation spectroscopy. In contrast to pure aluminum clusters, the vanadium doped clusters are reactive towards hydrogen, but in a size-dependent way. IR spectroscopy shows that for the most reactive cluster, $Al_{10}V^+$, the hydrogen dissociates upon adsorption but desorbs molecularly. For smaller Al_nV^+ clusters, density functional theory calculations demonstrate that the reactivity pattern is not so much the result of the energetics of the hydrogenation reaction as of the kinetics, with large activation barriers due to unfavorable/insufficient orbital overlap between cluster and molecular hydrogen orbitals. The decrease in reactivity for larger clusters with $n > 16$ is attributed to cage formation, in which the vanadium dopant occupies an endohedral position in the cluster. Our results confirm that transition metal doping of aluminum clusters improves their reactivity towards hydrogen, but that in the case of a single vanadium dopant only a narrow size range becomes active.

Methods Section

The bimetallic vanadium-aluminum clusters were produced in a dual laser ablation source setup which has been described in detail elsewhere[28]. Hydrogen was injected into the source by a separate valve. After formation, the clusters were extracted and detected in a reflectron time-of-flight mass spectrometer. Infrared light (800–2100 cm^{-1}, 50 mJ per pulse) produced by the free-electron laser of the Fritz-Haber-Institut der Max-Planck-Gesellschaft[29,30] was focused onto the clusters through a 2 mm aperture before extraction.

DFT calculations were performed in SIESTA[31], using the spin-polarized GGA-PBE[32] exchange-correlation functional. In SIESTA, core electrons were treated with norm-conserving scalar relativistic pseudopotentials in their fully non-local form[33], whereas for the valence electrons linear combinations of numerical pseudo-atomic orbitals (PAO) were used (double zeta polarized basis (DZP) set in this work). The equilibrium geometries resulted from an unconstrained conjugate-gradient structural relaxation using the DFT forces until the force on each atom was smaller than 0.001 eV/Å. The calculation of the dissociation barriers has been performed by the climbing nudged elastic band method[34] within the VASP[35] code. The IR spectra were calculated with the ORCA[36] code (GGA-PBE/def2-TZVP) after re-optimization of the SIESTA structures. The density of states and electronic orbitals were calculated with Quantum Espresso[37] (GGA-PBE, ultrasoft Vanderbilt core pseudopotentials, plane wave cutoff energy of 200 eV).

Acknowledgements

This work is supported by the KU Leuven Research Council (GOA/14/007). J.V. would like to thank the FWO – Research Foundation Flanders for a PhD fellowship. P.F. acknowledges CONICyT for a Becas Chile scholarship. A.F. thanks the Deutsche Forschungsgemeinschaft for a Heisenberg grant (FI 893/6).

Keywords: hydrogen storage • metal clusters • mass spectrometry • IR spectroscopy• density functional theory calculations • ion-molecule reactions

[1] S. Niaz, T. Manzoor, A. H. Pandith, *Renew. Sustain. Energy Rev.* **2015**, *50*, 457.

[2] G. W. Crabtree, M. S. Dresselhaus, M. V. Buchanan, *Phys. Today* **2004**, 39.

[3] D. J. Durbin, *Int. J. Hydrogen Energy* **2013**, *38*, 14595.

[4] M. Ball, M. Weeda, *Int. J. Hydrogen Energy* **2015**, *40*, 7903.

[5] P. Jena, *J. Phys. Chem. Lett.* **2011**, *2*, 206.

[6] L. Schlapbach, A. Züttel, *Nature* **2001**, *414*, 353.

[7] M. Felderhoff, C. Weidenthaler, R. von Helmolt, U. Eberle, *Phys. Chem. Chem. Phys.* **2007**, *9*, 2643.

[8] H. Schwarz, *Angew. Chem. Int. Ed.* **2015**, *54*, 10090; Angew. Chem. **2015**, 127, 10228.

[9] R. Zidan, B. L. Garcia-Diaz, C. S. Fewox, A. C. Stowe, J. R. Gray, A. G. Harter, *Chem. Commun.* **2009**, 3717.

[10] C. P. Baldé, B. P. C. Hereijgers, J. H. Bitter, K. P. de Jong, *J. Am. Chem. Soc.* **2008**, *130*, 6761.

[11] T. H. Upton, D. M. Cox, A. Kaldor, in *Phys. Chem. Small Clust.* (Eds.: P. Jena, B.K. Rao, S.N. Khanna), Springer, **1987**, pp. 755.

[12] I. Pino, G. J. Kroes, M. C. Van Hemert, *J. Chem. Phys.* **2010**, *133*, 184304.

[13] M. F. Jarrold, J. E. Bower, *Chem. Phys. Lett.* **1988**, *144*, 311.

[14] D. M. Cox, D. J. Trevor, R. L. Whetten, A. Kaldor, *J. Phys. Chem.* **1988**, *92*, 421.

[15] A. A. Mikhailin, O. P. Charkin, N. M. Klimenko, *Russ. J. Inorg. Chem.* **2012**, *57*, 528.

[16] I. S. Chopra, S. Chaudhuri, J. F. Veyan, Y. J. Chabal, *Nature Mater.* **2011**, *10*, 986.

[17] F. Zhang, Y. Wang, M. Y. Chou, *J. Phys. Chem. C* **2012**, *116*, 18663.

[18] L. Guo, Y. Yang, *Int. J. Hydrogen Energy* **2013**, *38*, 3640.
[19] S. Nonose, Y. Sone, K. Onodera, S. Sudo, K. Kaya, *Chem. Phys. Lett.* **1989**, *164*, 427.
[20] S. M. Lang, P. Claes, S. Neukermans, E. Janssens, *J. Am. Soc. Mass Spectrom.* **2011**, *22*, 1508.
[21] E. M. Fernández, A. Vega, L. C. Balbás, *J. Chem. Phys.* **2013**, *139*, 214305.
[22] S. Chaudhuri, J. Graetz, A. Ignatov, J. J. Reilly, J. T. Muckerman, *J. Am. Chem. Soc.* **2006**, *128*, 11404.
[23] O. P. Charkin, A. A. Mikhailin, N. M. Klimenko, *Russ. J. Inorg. Chem.* **2013**, *58*, 1479.
[24] A. Fielicke, A. Kirilyuk, C. Ratsch, J. Behler, M. Scheffler, G. von Helden, G. Meijer, *Phys. Rev. Lett.* **2004**, *93*, 23401.
[25] I. Swart, F. M. F. de Groot, B. M. Weckhuysen, P. Gruene, G. Meijer, A. Fielicke, *J. Phys. Chem. A* **2008**, *112*, 1139.
[26] I. Swart, P. Gruene, A. Fielicke, G. Meijer, B. M. Weckhuysen, F. M. F. de Groot, *Phys. Chem. Chem. Phys.* **2008**, *10*, 5743.
[27] J. Moc, *Chem. Phys. Lett.* **2008**, *466*, 116.
[28] A. Fielicke, G. von Helden, G. Meijer, *Eur. Phys. J. D* **2005**, *34*, 83.
[29] W. Schöllkopf, S. Gewinner, H. Junkes, A. Paarmann, G. von Helden, H. Bluem, A. M. M. Todd, in *Proc. SPIE*, **2015**, *9512,* p. 95121L.
[30] W. Schöllkopf, S. Gewinner, W. Erlebach, H. Junkes, A. Liedke, G. Meijer, A. Paarmann, G. von Helden, H. Bluem, D. Dowell, et al., in *Proc. FEL 2014*, Basel, Switzerland, **2014**, WEB04, pp. 629.
[31] J. M. Soler, E. Artacho, J. D. Gale, A. Garcia, J. Junquera, P. Ordejon, D. Sanchez-Portal, *J. physics. Condens. matter* **2002**, *14*, 2745.
[32] J. P. Perdew, K. Burke, M. Ernzerhof, *Phys. Rev. Lett.* **1996**, *77*, 3865.
[33] L. Kleinman, D. M. Bylander, *Phys. Rev. Lett.* **1987**, *48*, 1425.
[34] G. Henkelman, B. P. Uberuaga, H. Jónsson, *J. Chem. Phys.* **2000**, *113*, 9901.
[35] G. Kresse, J. Furthmüller, *Phys. Rev. B* **1996**, *54*, 11169.
[36] F. Neese, *Wiley Interdiscip. Rev. Comput. Mol. Sci.* **2012**, *2*, 73.
[37] P. Giannozzi, S. Baroni, N. Bonini, M. Calandra, R. Car, C. Cavazzoni, D. Ceresoli, G. L. Chiarotti, M. Cococcioni, I. Dabo, et al., *J. Phys. Condens. Matter* **2009**, *21*, 395502.